

An improvement in the nine-point central difference image correction method for digital particle image velocimetry recording evaluation

L Gui and J M Seiner

Jamie L Whitten National Center for Physical Acoustics (NCPA), University of Mississippi, University, MS 38677-1848, USA

Received 5 March 2004, in final form 7 July 2004

Published 20 August 2004

Online at stacks.iop.org/MST/15/1958

doi:10.1088/0957-0233/15/10/002

Abstract

A proper adjustment of the translation portion of pixel shifts for the multi-pass, nine-point (9P), central difference image correction (CDIC) method is found to be effective for further reducing the evaluation errors of digital particle image velocimetry recordings. In the improved central difference image correction scheme, the translation portion of pixel shifts is adjusted between the mean value of particle image displacements (initially introduced for the 9P method) and the particle image displacement at the centre (initially suggested for the four-point method) of the interrogation window, so that the evaluation errors of the iterated evaluation may converge to a lower level than both the initially introduced nine- and four-point methods. Based on a 50% overlap of interrogation windows, five possible algorithms to determine the pixel translation shift of the central difference image correction are discussed. Tests with synthetic particle image velocimetry recording pairs of simulated periodic flows demonstrate that the evaluation error of the 9P-central difference image correction method can be reduced to less than half of its initially introduced level, and it is obviously lower than that of the four-point method suggested by Wereley and Gui (2001 *4th Int. Symp. on Particle Image Velocimetry (Göttingen, Germany, 17–19 Sept.)*; 2003 *Exp. Fluids* **34** 42–51). Simulations and real image tests indicate that the error distribution and the peak-locking effect of the central difference image correction method have a two-pixel period.

Keywords: PIV, CDIC, image evaluation, image correction, peak-locking effect

Abbreviations

4P	four point
9P	nine point
CDI	central difference interrogation
CDIC	central difference image correction
CWS	continuous window shift
DWS	discrete window shift
CTR	correlation-based tracking algorithm
FDI	forward difference interrogation
FFT	fast Fourier transformation

PIV	particle image velocimetry
rms	root mean square

1. Introduction

In order to improve the evaluation quality of digital particle image velocimetry (PIV) recordings, window shift techniques have been used for many years (Keane and Adrian 1993, Willert 1996, Cowen and Monismith 1997, Westerweel *et al* 1997, Scarano and Riethmuller 1999). When a window shift is applied to the correlation-based interrogation algorithm,

i.e. correlating two equally sized image samples, big evaluation errors at large particle image displacements are avoided. When a window shift is used with the correlation-based tracking (CTR) algorithm, i.e. correlating a smaller image sample with a bigger one, a smaller window than usual may be adopted so that the spatial resolution can be increased. Since the evaluation errors (bias and random) of the correlation-based interrogation algorithm are extremely small around zero-particle image displacement, a multi-pass continuous window shift technique is used to greatly increase the evaluation accuracy of digital PIV recordings (Sjödahl 1994, Sholl and Savas 1997, Scarano and Riethmuller 2000, Gui and Wereley 2002). By the window shift, the position shifts of all the pixels in the interrogation window are the same, so that only the translation of the particle image pattern in the interrogation window is taken into account.

To account not only for the translation but also for the distortion of the particle image pattern resulting from complex flows, image pattern correction techniques were developed (Huang *et al* 1993, Tokumaru and Dimotakis 1995, Lin and Perlin 1998, Nogueira *et al* 1999, 2001, Scarano 2002). By the image pattern correction, the position shift is individually determined for each pixel in the interrogation window. The central difference image correction (CDIC) method was developed by Wereley and Gui (2001, 2003), that combines advantages of central difference interrogation (CDI) (Wereley *et al* 1998, Wereley and Meinhart 2000, 2001), continuous window shift (CWS) and image correction. The initially described CDIC is a multi-pass evaluation scheme that is constructed on the correlation-based interrogation algorithm with a 50% interrogation window overlap. Because of the 50% overlap of the interrogation window, previously determined particle image displacements at nine points, i.e. the centre, the four corners and the four sideline centres of the interrogation window, are available for determining the image pattern correction. Since the other image correction techniques are usually combined with the correlation-based tracking algorithm that needs much more computation time than the correlation-based interrogation algorithm, and they usually require a higher interrogation window overlap, the CDIC can be considered as the fastest one among the effective image pattern correction methods.

In order to completely use the information available by the 50% window overlap, i.e. the particle image displacements at the nine points determined in the previous iteration cycle of the multi-pass evaluation, the interrogation window is divided into four rectangular cells, and a bilinear interpolation is used in each cell to determine the shift of each pixel in the cell according to the four particle image displacements at the cell corners. The translation portion of the pixel shifts is determined by the mean displacement of the nine available points, whereas the differences between the mean displacement and the particle image displacements at the nine points determine the distortion portion of the pixel shifts. However, as presented by Wereley and Gui (2001, 2003), this nine-point (9P) algorithm seems not to be optimal, because a simplified algorithm that uses only particle image displacements at four corners of the interrogation window converges to a much lower evaluation error level. This implies that the 9P-CDIC can possibly be further improved.

In this paper, we shall first provide a mathematical description of the CDIC method and possible algorithms for adjusting the pixel shifts. Then synthetic particle images and simulated particle image displacements will be introduced and used to test these algorithms. This is followed by tests and discussions on the evaluation error distributions and the peak-locking effect.

2. Description of the method

2.1. Mathematical description of CDIC

For a single exposed PIV recording pair, the correlation-based interrogation algorithm is applied to two small image fractions (i.e. evaluation samples) of the same size. Traditionally, the two evaluation samples are chosen, respectively, from the first and second images in the PIV recording pair at the same position in the image coordinate. The evaluation (cross-correlation) function is simply given as

$$\Phi(m, n) = \sum_{i=1}^M \sum_{j=1}^N g_1(i, j) \cdot g_2(i + m, j + n) \quad (1)$$

where $g_1(i, j)$ and $g_2(i, j)$ are grey value distributions of the two evaluation samples, which are restricted in a rectangular interrogation window of size $M \times N$ pixels. The mean particle image displacement in the interrogation window is determined by the position of the maximal function value in the m - n plane. When the computation of evaluation function $\Phi(m, n)$ is accelerated by using the fast Fourier transformation (FFT) algorithm, $g_1(i, j)$ and $g_2(i, j)$ are assumed as being distributed periodically in the i - j plane with the periodicity M, N . The grey value distributions of the evaluation samples $g_1(i, j), g_2(i, j)$ are related to the grey value distributions of the whole PIV recordings $G_1(x, y), G_2(x, y)$ as

$$\begin{aligned} g_1(i, j) &= G_1\left(x_0 - \frac{M}{2} + i, y_0 - \frac{N}{2} + j\right) \\ g_2(i, j) &= G_2\left(x_0 - \frac{M}{2} + i, y_0 - \frac{N}{2} + j\right), \end{aligned} \quad (2)$$

where (x_0, y_0) is the evaluation point in PIV recordings. When pixel shifts $(x_{\text{pix1}}, y_{\text{pix1}})$ and $(x_{\text{pix2}}, y_{\text{pix2}})$ are applied to the first and second images of the PIV recording pairs, respectively, the relations between evaluation samples and PIV recordings become

$$\begin{aligned} g_1(i, j) &= G_1\left(x_0 + x_{\text{pix1}} - \frac{M}{2} + i, y_0 + y_{\text{pix1}} - \frac{N}{2} + j\right) \\ g_2(i, j) &= G_2\left(x_0 + x_{\text{pix2}} - \frac{M}{2} + i, y_0 + y_{\text{pix2}} - \frac{N}{2} + j\right). \end{aligned} \quad (3)$$

When the pixel shifts are constants in the interrogation window, equation (3) represents window shifting techniques as below:

- DWS: $x_{\text{pix1}}, y_{\text{pix1}}, x_{\text{pix2}}, y_{\text{pix2}}$ are integer numbers;
- CWS: $x_{\text{pix1}}, y_{\text{pix1}}, x_{\text{pix2}}, y_{\text{pix2}}$ are not integers;
- FDI: $x_{\text{pix1}} = 0, y_{\text{pix1}} = 0$;
- CDI: $x_{\text{pix1}} = -x_{\text{pix2}}, y_{\text{pix1}} = -y_{\text{pix2}}$.

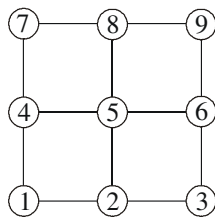


Figure 1. Available evaluation points on an interrogation window with 50% overlap.

For the CDIC evaluation scheme, the pixel shifts are functions of each pixel (i, j) in the interrogation window, and they are determined by

$$\begin{cases} x_{\text{pix1}}(i, j) = -\frac{1}{2}x_t - \frac{1}{2}x_d(i, j) \\ y_{\text{pix1}}(i, j) = -\frac{1}{2}y_t - \frac{1}{2}y_d(i, j) \\ x_{\text{pix2}}(i, j) = \frac{1}{2}x_t + \frac{1}{2}x_d(i, j) \\ y_{\text{pix2}}(i, j) = \frac{1}{2}y_t + \frac{1}{2}y_d(i, j), \end{cases} \quad (4)$$

where the translation shift (x_t, y_t) is constant in the interrogation window, whereas the distortion shift (x_d, y_d) varies from pixel to pixel. Theoretically, the translation shift should be the mean pixel shift in the interrogation window, and the integration of the distortion function should be zero, i.e.

$$\begin{cases} \sum_{i=1}^M \sum_{j=1}^N x_d(i, j) = 0 \\ \sum_{i=1}^M \sum_{j=1}^N y_d(i, j) = 0. \end{cases} \quad (5)$$

Since the grey value distributions in the digital PIV images are not continuous functions, an interpolation is usually required to complete equation (3), except for discrete window shift (DWS).

2.2. Pixel shifts and adjustments

As shown in figure 1, nine evaluation points are set on an interrogation window, when a 50% overlap is used. In the multi-pass CDIC scheme, the evaluated particle image displacements at the nine points, i.e. $\{(\Delta x_k, \Delta y_k), k = 1, 2, \dots, 9\}$, are determined after an evaluation run, and they are then used to determine the image pattern translation (x_t, y_t) and distortion $(x_d(i, j), y_d(i, j))$ in the next evaluation run. As such, the evaluation is iterated until a convergence condition is fulfilled. As described by Wereley and Gui (2003), four or five iterations are usually necessary for using CDIC to get an accurate, converged result. Ten iterations are applied in the following tests to obtain fully converged evaluation results.

The distortion shifts at the nine points are determined as

$$\begin{cases} x_d(k) = \Delta x_k - \overline{\Delta x} \\ y_d(k) = \Delta y_k - \overline{\Delta y}, \end{cases} \quad (6)$$

wherein $(\overline{\Delta x}, \overline{\Delta y})$ is the mean value of the particle image displacements at the nine points. The distortion shift of other pixels in the window is determined with a bilinear interpolation in the rectangular cells according to the values determined with equation (6). In the initially introduced CDIC (Wereley and Gui 2001, 2003), the translation shift is

determined by the mean displacement, i.e.

$$\text{Algorithm 0: } \begin{cases} x_t = \overline{\Delta x} \\ y_t = \overline{\Delta y}. \end{cases} \quad (7)$$

It seems also reasonable to determine the translation shift with the particle image displacement at the window centre, i.e.

$$\text{Algorithm 5: } \begin{cases} x_t = \Delta x_5 \\ y_t = \Delta y_5. \end{cases} \quad (8)$$

Four adjustments of the translation shift may be made between $(\overline{\Delta x}, \overline{\Delta y})$ and $(\Delta x_5, \Delta y_5)$ as below.

Algorithm 1:

$$\begin{cases} x_t = \overline{\Delta x} + \Delta x_5 - \frac{\Delta x_2 + \Delta x_4 + \Delta x_6 + \Delta x_8}{4} \\ y_t = \overline{\Delta y} + \Delta y_5 - \frac{\Delta y_2 + \Delta y_4 + \Delta y_6 + \Delta y_8}{4} \end{cases} \quad (9)$$

Algorithm 2:

$$\begin{cases} x_t = \overline{\Delta x} + \Delta x_5 - \frac{\Delta x_1 + \Delta x_3 + \Delta x_7 + \Delta x_9}{4} \\ y_t = \overline{\Delta y} + \Delta y_5 - \frac{\Delta y_1 + \Delta y_3 + \Delta y_7 + \Delta y_9}{4} \end{cases} \quad (10)$$

Algorithm 3:

$$\begin{cases} x_t = \overline{\Delta x} + \Delta x_5 - \frac{\Delta x_2 + \Delta x_4 + \Delta x_5 + \Delta x_6 + \Delta x_8}{5} \\ y_t = \overline{\Delta y} + \Delta y_5 - \frac{\Delta y_2 + \Delta y_4 + \Delta y_5 + \Delta y_6 + \Delta y_8}{5} \end{cases} \quad (11)$$

Algorithm 4:

$$\begin{cases} x_t = \overline{\Delta x} + \Delta x_5 - \frac{\Delta x_1 + \Delta x_3 + \Delta x_5 + \Delta x_7 + \Delta x_9}{5} \\ y_t = \overline{\Delta y} + \Delta y_5 - \frac{\Delta y_1 + \Delta y_3 + \Delta y_5 + \Delta y_7 + \Delta y_9}{5}. \end{cases} \quad (12)$$

For the initially suggested four-point CDIC method, $(\Delta x_1, \Delta y_1)$, $(\Delta x_3, \Delta y_3)$, $(\Delta x_7, \Delta y_7)$ and $(\Delta x_9, \Delta y_9)$ are used to determine the distortion shift with equation (6), and $(\Delta x_5, \Delta y_5)$ used to determine the translation shift, i.e. equation (8). Note that equations (8) and (10) are identical for the 4P method. An alternative for the 4P-CDIC is to use equation (12). Since the initially suggested CDIC method involves five points ($k = 1, 3, 5, 7, 9$), it can also be called five-point CDIC. It was named four-point CDIC, because only four points ($k = 1, 3, 7, 9$) are used in equation (6) to determine the distortion shift.

3. Tests of CDIC algorithms

The above-mentioned CDIC algorithms are tested here by using synthetic particle images and simulated flows, so that the evaluation errors can be quantitatively discussed.

3.1. Synthetic PIV images

The intensity distribution of a synthetic particle image is simulated to have a Gaussian profile, i.e.

$$I_k(x, y) = B_k \exp\left(-2\frac{(x - x_k)^2 + (y - y_k)^2}{d_k^2}\right) \quad (13)$$

where number k indicates the particle image at position (x_k, y_k) , B_k is the intensity (brightness) at the particle image centre and d_k is the particle image diameter. To account for

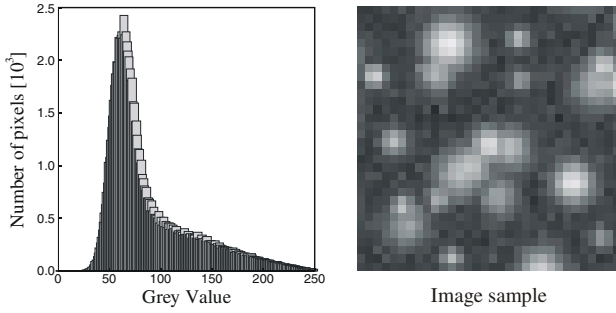


Figure 2. Histogram (left) and sample (right) of a synthetic PIV image.

thermal noise in the CCD array, single-pixel random noise $I_{sp}(x, y)$ is synthetically generated so that

$$I_{sp}(x, y) = I_0 + I_r(x, y) \quad (14)$$

where I_0 is the mean value, and $I_r(x, y)$ is the random portion that has a Gaussian probability density distribution. The intensity of the single-pixel random noise is quantified with

$$I_{rms} = \sqrt{\frac{1}{HW} \sum_{y=1}^H \sum_{x=1}^W I_r^2(x, y)}, \quad (15)$$

where H and W are the height and width of the image frame, respectively. The grey value distribution of the synthetic PIV image is finally determined by

$$G(x, y) = \sqrt{I_{sp}^2(x, y) + \sum_{k=1}^P I_k^2(x, y)} \quad (16)$$

where P is the total number of particle images that are randomly distributed in the image frame. In the tests conducted in this paper, synthetic particle images are generated in a frame of 1024×1024 pixels with average particle image number 20 in a 32×32 -pixel window. The particle image diameter and brightness are randomly distributed in given regions, i.e. $d = 2-5$ and $B = 130-250$. The single-pixel random noise of $I_0 = 60$ and $I_{rms} = 10$ is superimposed onto the synthetic PIV images. The histogram of one of the synthetic PIV images and an image sample of 32×32 pixels are shown in figure 2. The histogram and the particle image pattern look reasonable, i.e. very similar to those of real PIV recordings. Note that no missing particles have been considered between one frame and the other in the following tests.

3.2. Test of 9P-CDICs using periodical flow pattern

In order to investigate the influence of the particle image pattern distortion on the evaluation errors of the CDIC algorithms, a periodical distribution of particle image displacements is simulated as

$$\begin{cases} \Delta x(x, y) = A \cos(2\pi y/\lambda) \\ \Delta y(x, y) = A \cos(2\pi x/\lambda) \end{cases} \quad (17)$$

where A is the amplitude, and λ is the wavelength. Both the amplitude and the wavelength can be used to adjust the strength of the image pattern distortion.

In the first test the magnitude A is given as 5 pixels, and the wavelength λ varies from 128 to 512 pixels in seven steps.

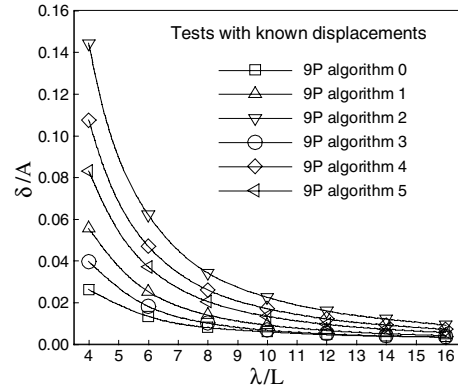


Figure 3. Influence of wavelength on evaluation error by correcting image with known displacements.

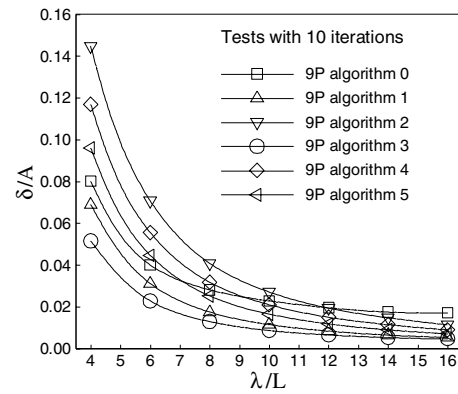


Figure 4. Influence of wavelength on evaluation error by correcting image with iterations.

The evaluations of the seven synthetic PIV recording pairs are conducted using a 32×32 -pixel interrogation window with a 50% overlap. A root-mean-square (rms) error (δ) is computed with about 4000 vectors obtained for each PIV recording pair. The test is carried out in two steps: first, the evaluation is not iterated, and the particle image pattern correction is performed with known (true) particle image displacements; second, the evaluation is iterated ten times for a fully converged result, and the displacements are set to zero at the beginning. According to equations (7)–(12), six 9P-CDIC algorithms are tested.

Figure 3 shows the influence of the spatial wavelength of the periodically distributed particle image displacements on the rms evaluation errors for correcting the particle image pattern with known displacements. The test results in figure 3 illuminate that the rms errors decrease with increasing wavelength and that the initially introduced 9P-CDIC algorithm, i.e. ‘9P algorithm 0’, has a lower error level than the other five algorithms, and that ‘9P algorithm 3’ performs the second best in this ideal case.

The errors of iterated evaluations are given in figure 4. It is shown that ‘9P algorithm 0’ no longer performs the best among the six algorithms in the iterated evaluation scheme, i.e. its error level is higher than those of algorithms 1 and 3 at short wavelengths, and higher than all others at long wavelengths. ‘9P algorithm 3’ becomes the best overall in the tested wavelength region.

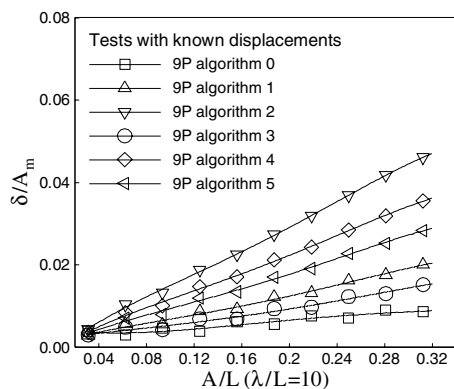


Figure 5. Influence of amplitude on evaluation error by correcting image with known displacements.

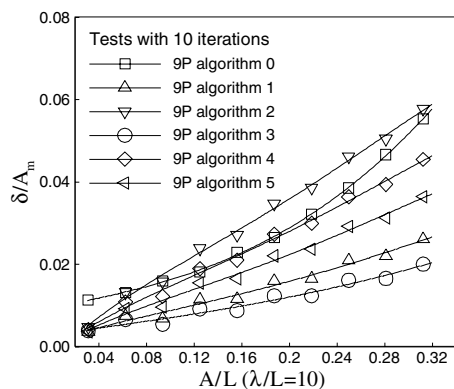


Figure 6. Influence of amplitude on evaluation error by correcting image with iterations.

The second test is conducted with a fixed wavelength, i.e. $\lambda = 320$ pixels, whereas the amplitude A varies from 1 to 10 pixels. The same as in the first test, the evaluations are conducted using a 32×32 -pixel interrogation window with a 50% overlap. For each simulated PIV recording pair about 4000 displacement vectors are used to determine the rms error. Results are given in figures 5 and 6 for correcting a particle image pattern with known and iterated values, respectively. It is also found in the second test that the ‘9P algorithm 0’ only performs the best when known displacements are used to correct the image pattern. When iterations are applied, ‘9P algorithm 3’ achieves the lowest error level.

It can be seen in all the above test results (figures 3–6) that the evaluation error is very sensitive to the algorithm chosen to determine the translation shift, especially in cases of small wavelengths and large amplitudes of periodical particle image displacement distributions.

According to the above discussions, it can be concluded that even through ‘9P algorithm 0’ is based on the theoretical definition of the translation and distortion shift (see section 2.1) and performs the best with true particle image displacements at the nine points, it does not work very well in an iterated evaluation scheme for real PIV recordings, where the true particle image displacement is unknown at any pixel in the interrogation window. It can be explained that the iterated evaluation is a numerical approach that usually converges to an approximation solution that deviates from the true solution.

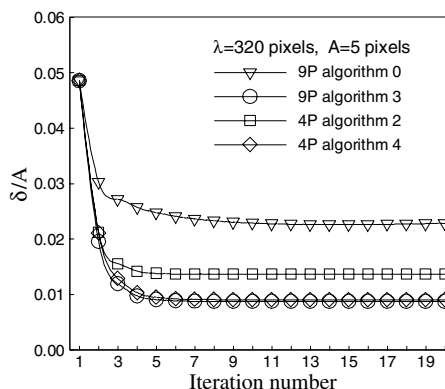


Figure 7. Evaluation errors of four different CDIC algorithms.

The deviation of the converged approximation solution may usually be effectively reduced by modifying the temporal solution between iterations with a certain method. In this work, five possible methods are tested with simulated complex flows, and ‘9P algorithm 3’ seems to be the most effective.

3.3. Comparison between 9P- and 4P-CDIC

The third test is conducted with a fixed wavelength magnitude, i.e. $\lambda = 320$ pixels, and a fixed amplitude, i.e. $A = 5$ pixels. Two four-point-CDIC (4P-CDIC) algorithms are added to this test for comparison: (1) ‘4P algorithm 2’ determines the translation shift with equation (10), which is the algorithm suggested by Wereley and Gui (2001, 2003); (2) ‘4P algorithm 4’ determines the translation shift with equation (12). The evaluations are iterated 20 times using a 32×32 -pixel interrogation window with a 50% overlap. RMS evaluation errors of each iteration for ‘9P algorithm 0’, ‘9P algorithm 3’, ‘4P algorithm 2’ and ‘4P algorithm 4’ are given in figure 7.

Figure 7 confirms the discussions in Wereley and Gui (2001, 2003), i.e. that the initially introduced 4P algorithm (4P algorithm 2) converges to an obviously lower error level than the initially introduced 9P algorithm (9P algorithm 0). Apparently, the errors of both ‘9P algorithm 3’ and ‘4P algorithm 4’ converge to even lower error levels. In the current test ‘9P algorithm 3’ performs a little better than ‘4P algorithm 4’. In fact the latter is the best of the possible 4P algorithms. The detailed discussions on the 4P algorithms are omitted. Figure 7 also shows that the evaluation errors of all the tested CDIC algorithms converge after six iterations. According to the above discussions, ‘9P algorithm 3’ is suggested as an improved 9P-CDIC method to replace ‘4P algorithm 2’.

4. Error distributions and peak locking

4.1. Error distributions of CDIC

In order to investigate the error distributions of the improved 9P-CDIC method, 61 synthetic PIV recording pairs of uniform particle image displacements varying from 0 to 6 pixels with a step of 0.1 pixels are used in the test. This test is carried out for ‘9P algorithm 3’ in two cases: (1) evaluation without iteration, (2) evaluation with ten iterations. The evaluations are conducted using a 32×32 -pixel interrogation window with

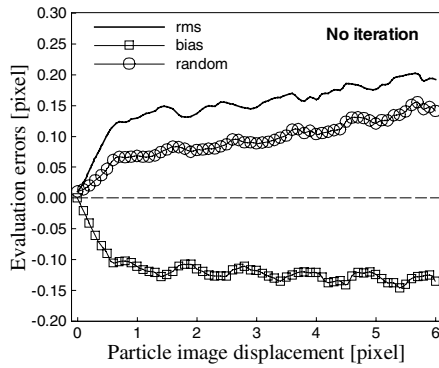


Figure 8. Evaluation error distributions on particle image displacement for evaluation without iterations.

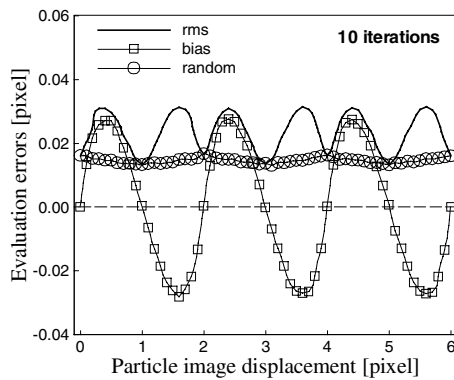


Figure 9. Evaluation error distributions on particle image displacement for evaluation with ten iterations.

a 50% overlap. The distributions of the bias error, random error and the rms error (i.e. total error) for the case without iteration are given in figure 8. It displays a typical dependence of evaluation errors of the correlation-based interrogation algorithm on the particle image displacement. Test results with ten iterations are given in figure 9. The figure indicates a two-pixel period in the periodical distributions of bias and random errors. In comparison to figure 8, the rms evaluation error of the iterated evaluation is much smaller than that of the evaluation without iteration. The two-pixel period of the error distributions can be explained as a feature of CDIC, because the pixels of the two evaluation samples in the interrogation window are continuously shifted in two opposite directions.

4.2. Peak-locking effect of CDIC

Since the period of the bias and random error distributions of CDIC is two pixels, and the error distributions determine the peak-locking effect (Gui and Wereley 2002), the two-pixel period should be reflected in the distribution density function, i.e. histogram, of the evaluated particle image displacements. In order to investigate the influence of the two-pixel error period of CDIC on the peak-locking effect, 100 pairs of PIV recordings taken in a turbulent jet flow are used for a test (Fukushima *et al* 2002, Westerweel *et al* 2002). The histogram and an image sample are given in figure 10. Since the particle images are very small and far from a Gaussian shape, a very strong peak-locking effect will be encountered in the evaluation results of some conventional evaluation methods, e.g. DWS and CTR.

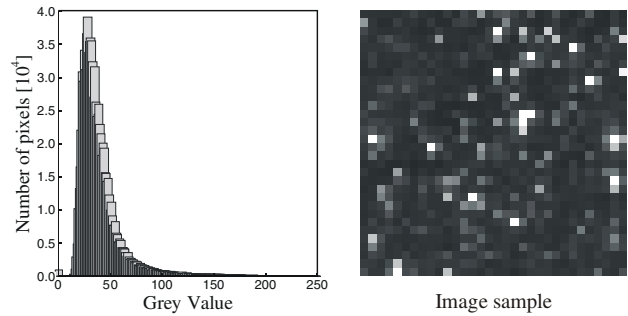


Figure 10. Histogram (left) and sample (right) of a real PIV recording.

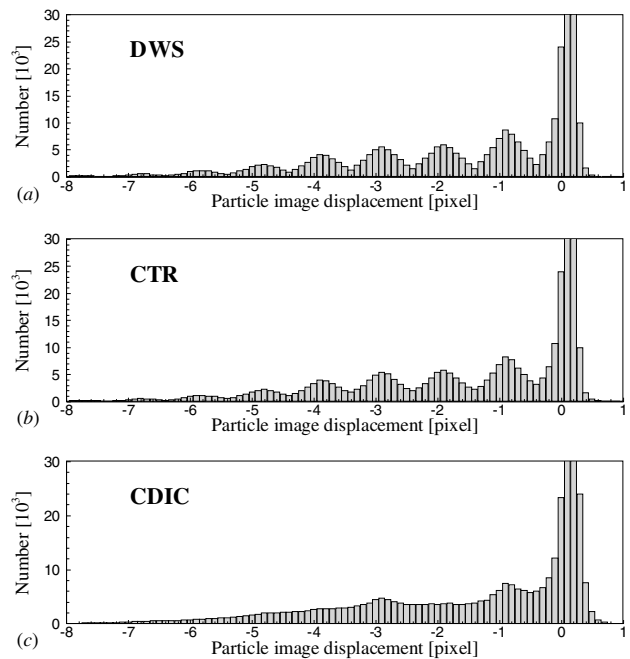


Figure 11. Histograms of the horizontal components of particle image displacements in PIV recordings taken in a turbulent jet flow.

These PIV recording pairs are evaluated with three evaluation algorithms: (1) correlation-based interrogation algorithm with discrete window shift, (2) correlation-based tracking algorithm (CTR), (3) improved 9P-CDIC (i.e. 9P algorithm 3). The histograms of the horizontal (jet axis direction) components of the particle image displacements are shown in figure 11. A very strong peak-locking effect is encountered in the evaluation results of both DWS and CTR (see figures 11(a) and (b)). The peak-locking effect of CDIC is much less than that of the other two algorithms (see figure 11(c)). Two non-natural peaks can be observed in the histogram for CDIC at a particle image displacement of -3 and -1 pixel, respectively, that verify a two-pixel period of the peak-locking effect.

5. Summary and conclusions

In order to improve the nine-point, central difference image correction (9P-CDIC) method, six possible algorithms for determining the translation pixel shift according to particle

image displacements at nine available points are discussed. Test results with simulated periodical particle image displacement distributions demonstrate that the evaluation error is very sensitive to the chosen algorithm for determining the translation pixel shift, especially at short wavelength and large amplitude of the distortion.

The initially introduced 9P-CDIC algorithm has the lowest evaluation error level among algorithms discussed in this paper when the true particle image displacement is used to correct the distorted particle image pattern; however, it does not perform well in the iterated evaluation scheme. Test results indicate that when the translation portion of the pixel shifts is adjusted with a algorithm described in this paper, i.e. '9P algorithm 3' determined by equation (11), the evaluation error of the multi-pass, 9P-CDIC method achieves the lowest evaluation error level. Further tests illuminate that '9P algorithm 3' performs much better than the initially suggested 4P-CDIC algorithm (4P algorithm 2) and also better than the improved 4P-CDIC algorithm (4P algorithm 4). Tests also demonstrate that the iterations of all the tested CDIC algorithms converge after six iterations.

The bias and random error distributions of CDIC have a period of two pixels on the particle image displacement. The two-pixel period feature of CDIC can be observed in the peak-locking effect of the evaluated particle image displacements when particle images are small or far from the Gaussian shape. A test with a set of real PIV recording pairs shows that CDIC has much less peak-locking effect than the currently widely used correlation-based tracking algorithm.

According to tests and discussions in this paper, the authors would like to suggest that '9P algorithm 3' is an improved 9P-CDIC method to replace the 4P-CDIC algorithm recommended by Wereley and Gui (2001, 2003).

Acknowledgments

Special thanks to Professor Jerry Westerweel, Delft University of Technology, the Netherlands, for providing experimental images of a turbulent jet flow.

References

Cowen E A and Monismith S G 1997 A hybrid digital particle tracking velocimetry technique *Exp. Fluids* **22** 199–211
 Gui L and Wereley S T 2002 A correlation-based continuous window shift technique for reducing the peak locking effect in digital PIV image evaluation *Exp. Fluids* **32** 506–17

Fukushima C, Aanen L and Westerweel J 2002 Investigation of the mixing process in an axisymmetric turbulent jet using PIV and LIF *Laser Techniques for Fluid Mechanics* ed R J Adrian *et al* (Berlin: Springer) pp 339–56
 Huang H T, Fiedler H E and Wang J J 1993 Limitation and improvement of PIV: II. Particle image distortion, a novel technique *Exp. Fluids* **15** 263–73
 Keane R D and Adrian R J 1993 Theory and simulation of particle image velocimetry *Laser Anemometry Advances Applications: 5th Int. Conf. (Veldhoven, The Netherlands, 23–27 August)* *Proc. SPIE* **2052** 477–92
 Lin H J and Perlin M 1998 Improved methods for thin, surface boundary layer investigations *Exp. Fluids* **25** 431–44
 Nogueira J, Lecuona A and Rodriguez P A 1999 Local field correction PIV: on the increase of accuracy of digital PIV systems *Exp. Fluids* **27** 107–16
 Nogueira J, Lecuona A and Rodriguez P A 2001 Local field correction PIV, implemented by means of simple algorithms, and multigrid versions *Meas. Sci. Technol.* **12** 1911–21
 Scarano F 2002 Iterative image deformation methods in PIV *Meas. Sci. Technol.* **13** R1–19
 Scarano F and Riethmuller M L 1999 Iterative multigrid approach in PIV image processing with discrete window offset *Exp. Fluids* **26** 513–23
 Scarano F and Riethmuller M L 2000 Advances in iterative multi-grid PIV image processing *Exp. Fluids* **29** 51–60
 Sholl M J and Savas Ö 1997 A fast Lagrangian PIV method for study of general high gradient flow *35th AIAA Aerospace Science Meeting (Reno, NV, 6–9 Jan.) AIAA Paper* 97-0493 (A97-15543)
 Sjö Dahl M 1994 Electronic speckle photography: increased accuracy by nonintegral pixel shift *Appl. Opt.* **33** 6667–73
 Tokumaru P T and Dimotakis P T 1995 Image correlation velocimetry *Exp. Fluids* **19** 1–15
 Wereley S T and Gui L 2001 PIV measurement in a four-roll-mill flow with a central difference image correction (CDIC) method *4th Int. Symp. on Particle Image Velocimetry (Göttingen, Germany, 17–19 Sept.)*
 Wereley S T and Gui L 2003 A correlation-based central difference image correction (CDIC) method and application in a four-roll-mill flow PIV measurement *Exp. Fluids* **34** 42–51
 Wereley S T and Meinhart C D 2000 Accuracy improvements in particle image velocimetry *10th Int. Symp. on Applications of Laser Techniques to Fluid Mechanics (Lisbon, Portugal, July)*
 Wereley S T and Meinhart C D 2001 Second-order accurate particle image velocimetry *Exp. Fluids* **31** 258–68
 Wereley S T, Santiago J G, Meinhart C D and Adrian R J 1998 Velocimetry for MEMS applications *Proc. of ASME/DSC (Micro-Fluidics Symposium) (Anaheim, CA, Nov. 1998)* vol 66
 Westerweel J, Dabiri D and Gharib M 1997 The effect of a discrete window offset on the accuracy of cross-correlation analysis of digital PIV recordings *Exp. Fluids* **23** 20–8
 Westerweel J, Hofmann T, Fukushima C and Hunt J C R 2002 The turbulent/non-turbulent interface at the outer boundary of a self-similar turbulent jet *Exp. Fluids* **33** 873–8
 Willert C E 1996 The fully digital evaluation of photographic PIV recordings *Appl. Sci. Res.* **56** 79–102